29 May 2010, 8:00 am - 9:30 am

3-D Modeling of Shear-Wave Velocity for Numerical Green's Function in Near-Field Ground Motion Simulation

Xiaodan Sun
Harbin Institute of Technology, China

Xiaxin Tao
Harbin Institute of Technology, China

Lijun Yin
China Railway Siyuan Survey and Design Group Co., Ltd., China

Dongli Zhang
Institute of Geology, CEA, China

Fifth International Conference on
Recent Advances in Geotechnical Earthquake Engineering and Soil Dynamics
and Symposium in Honor of Professor I.M. Idriss
May 24-29, 2010 • San Diego, California

3-D MODELING OF SHEAR-WAVE VELOCITY FOR NUMERICAL GREEN'S FUNCTION IN NEAR-FIELD GROUND MOTION SIMULATION

Xiaodan Sun[1], Xiaxin Tao[1], Lijun Yin[2], Dongli Zhang[3]
(1.Harbin Institute of Technology, Harbin, Heilongjiang 150090, China; China Railway Siyuan Survey and Design Group Co., LTD, Fuzhou, Fujian350013, China; 3. Institute of Geology, CEA, Beijing 100029, China)

ABSTRACT

Numerical Green's function is effective for simulating low-frequency ground motions in the near field, in which the whole computing region is divided into a homogenous zone including the source and an inhomogeneous zone (named overburden layer) from the ground surface to a certain depth. In this paper, a procedure to build a 3-D model that properly describes the shear-wave velocity structure of overburden layer and the topography of ground surface was presented. In this procedure, the overburden layer is discretized into finite elements based on the topography of ground surface and buried rock surface; shear-wave velocity data from inversion, surveying line and borehole are assigned to elements according to their locations in the overburden layer. For elements without available velocity data, a Kriging interpolation method based on the spherical variation function model was employed, and dummy borehole is also used to improve the validity of the interpolation based on sparse data. Particularly, block interpolation and interface smooth was suggested for computing region that contains several different geological conditions, such like a sedimentary basin and its vicinity. As an example, the 3-D shear-wave velocity of the Lanzhou sedimentary basin and its vicinity in Gansu, China was modeled using the procedure. Low-frequency ground motions at 10854 surface points in this region was simulated by Numerical Green's function based on this velocity model, among which ground motions at 7 representative points were compared with those simulated based on horizontal layered velocity model.

INTRODUCTION

The soil in a sediment basin near ground surface is soft. It has a remarkable amplification and filtering effects on earthquake wave and can change the characters of the amplitude and spectrum of ground motion wave significantly. This amplification and filtering mainly depends on the shear wave velocity structure in the basin. For the ground motion forecast of a basin, a proper 3D model that can reflect the real velocity structure of the earth crust and the wavy terrain of the ground surface and the buried rock surface is needed to ensure the reliability and accuracy of the numerical simulation. Many studies have been presented focusing on the modelling of velocity structure in the shallow crust (Magistrale, 1996; Graves, 1998; Olsen, 2000; Zhang, 2007). Most of these studies present a horizontal layered velocity structure which is considerably gross for the site where the sedimentary formation has large difference in properties in horizontal direction, such as the Lanzhou basin used in this paper. The Lanzhou basin is a slender Cenozoic basin covering a large area including three terraces around Huanghe River and loess terrace around the basin and the rock area. Shear-wave velocity for these regions is significantly different, which cannot be represented by a simple horizontal layered velocity structure.

NUMERICAL GREEN'S FUNCTION

Numerical Green's function was developed to simulate ground motions in low frequencies from finite faults. In this method, the whole computing region (from the ground surface to the lower boundary of the fault) is defined to be two parts, as figure 1 illustrated, the homogenous zone around the fault and the inhomogeneous zone from the ground surface to a certain depth, so called overburden layer. The 3D simulation of low-frequencies strong ground motion is then divided into two steps. Firstly, displacement time histories for each node on the bottom of discrete overburden layer caused by each sub-fault is calculated by the space-time convolution of the rise time of each sub-fault and 3-order Green function obtained from the superimposition of 9 Green functions of the corresponding 9 earthquake moment tensors, as shown in (2.1). Afterwards, displacement time histories of all sub-faults for each node are superimposed to provide the input for the following finite element numerical simulation. Secondly, displacement time histories for other nodes of discrete overburden layer are calculated by the space-time decoupling explicit finite element simulation with the aim of the second-order local artificial transmitting boundary.

$$F_P \times G_{np} = \sum_{i=1}^{m}\sum_{j=1}^{n} F_{\varsigma} \times G_{\varsigma\eta} \qquad (1)$$

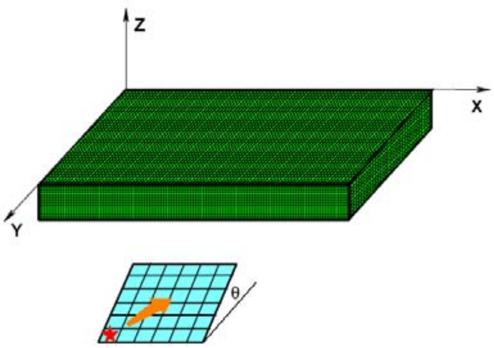

Fig. 1. Computing model for numerical Green function.

3D VELOCITY MODELING

The key issue for numerical Green's function is to specify a proper model to describe the inhomogeneity of the soil in the overburden layer. The authors develop a procedure to build three-dimensional velocity structure for overburden layer, in which velocity data from boreholes, survey lines and earthquake network were employed. The first step of the procedure is discretizing the overburden layer into finite elements. The dimension of finite element decides the accuracy of the numerical simulation. Theoretically, the smaller grid, the more accurate simulation. However, the overburden layer should extend enough in horizontal direction in order to neglect the effects of the incident wave on the lateral faces, which generally gives the overburden layer a very large dimension in horizontal direction. Considering the computing capacity of computers, the size of the grid is usually taken as several meters. Based on the grid size of hundreds of meters, frequencies greater than 2 Hz are not accurately synthesized (Archuleta and Frazier, 1978). Unlike the horizontal direction, the soil property in the vertical direction in the upper few kilometers changes rapidly. Therefore, the size of the grid in the vertical direction should be more detailed. Taking the Lanzhou basin as an example, the Lanzhou basin, Gansu, China, is a slender Cenozoic basin as figure 2 shows. In 2007, the authors preformed a project of the near-field ground

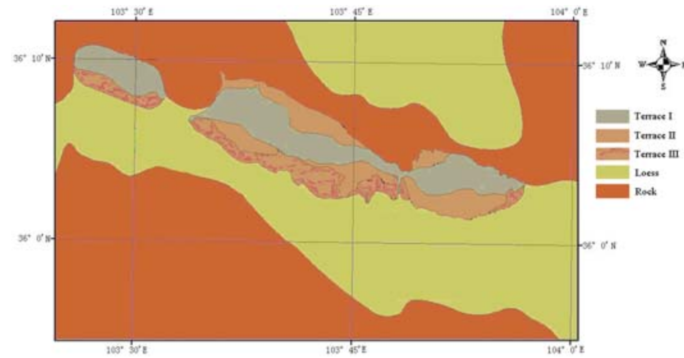

Fig. 2. Geological zone of the working area.

motion forecast of Lanzhou city and its vicinity from the given earthquake caused by Maxianshan Northern fault. In that project, the whole area shown in figure 2 with the dimension of 53.2 km×32 km was defined to be the working region, and the velocity structure model of the working region worked out by Shi (2007) is shown in figure 3. The model in figure 3 was built up based on data from boreholes and survey lines, but the problem for its application to numerical Green's function is that the total height of the model is 900 m which is much smaller than the vertical size of the overburden layer needed by numerical Green's function. Therefore, in our procedure, we defined a discretized overburden layer first to match the requirement of numerical Green's function and then assigned shear-wave velocity into each finite element of the overburden layer to form the 3D velocity model.

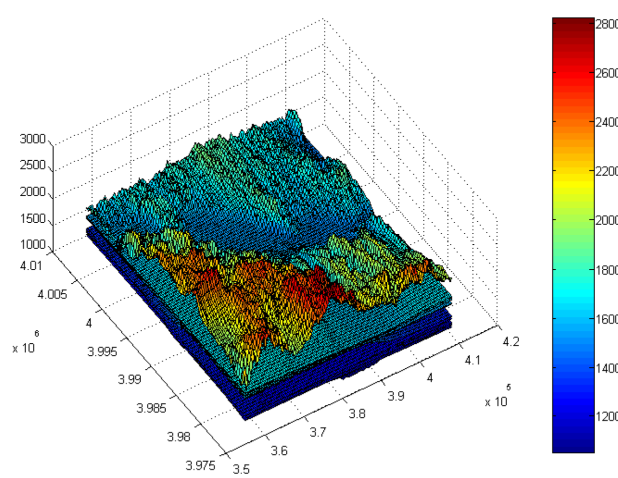

Fig.3. 3D velocity structure model for Lanzhou basin

For the Lanzhou basin, the grid size in horizontal direction was taken as 400km, and the grid size in vertical direction is inhomogeneous and depends on the terrace of the working region. In detail, we defined the thickness for rest layers is given by

$$\Delta H_v = \frac{H - \Delta H_1 - \Delta H_2}{n} \qquad (2)$$

Where H is the thickness of the overburden layer which depends on the ground terrace. ΔH_1 and ΔH_2 are the thickness of the first and second layer which are taken as 100km and 200km for the Lanzhou basin. n is the number of the layer which should be specified to make ΔH approach 400km. The 3D discretized model of the overburden layer for the Lanzhou basin is illustrated figure 4.

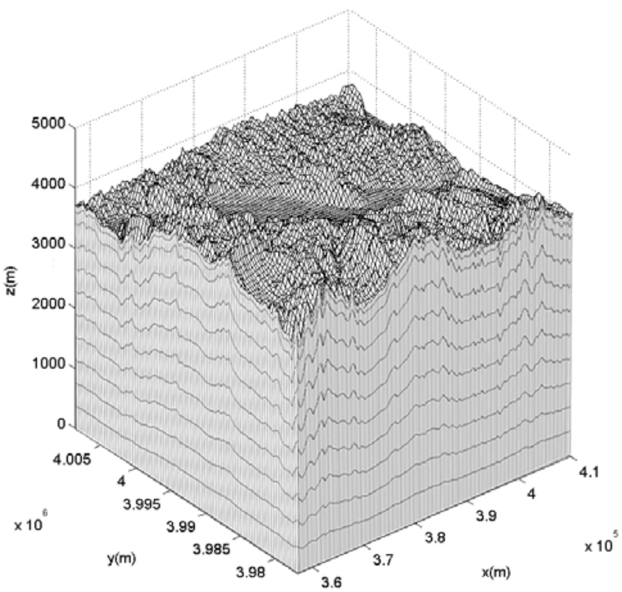

Fig. 4. 3D finite element model of the working area

The next step is to assign shear-wave velocity to the hollow finite element. For the Lanzhou basin, data from local inversion, surveying line and borehole were employed. Before assignment, data collected by Lanzhou Earthquake Administration were complemented based on some other geological exploration data.

In this project, there are 383 boreholes were used, in which 153 reach buried rock. Most of boreholes are distributed in Chengguan district, Anning district and Qilihe district of Lanzhou city as figure 5 shows. Velocity data at each borehole were then assigned to the hollow model according to the relative location of the borehole in the model as figure 6 illustrated. Most of these boreholes located in the depth from several meters to a hundred meter, only three deep boreholes has depth more than 600 hundred meters, which means only very few elements in the model could get velocity data after the assignment.

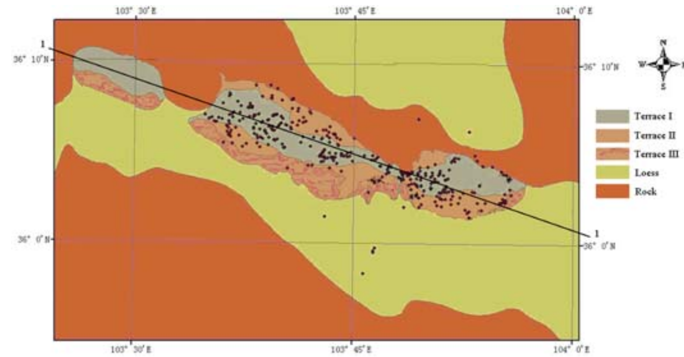

Fig.5. Plan for locations of boreholes

Due to the density of the boreholes and the element size, it's possible that several boreholes data are assigned to one element. For this case, the mean of these data was taken as the velocity of the element. The structure model in figure 5 after assignment with borehole data was illustrated in figure 7. The profile of section 1-1 in figure 5 is shown in figure 8 for clearly showing the inner structure of the model after assignment.

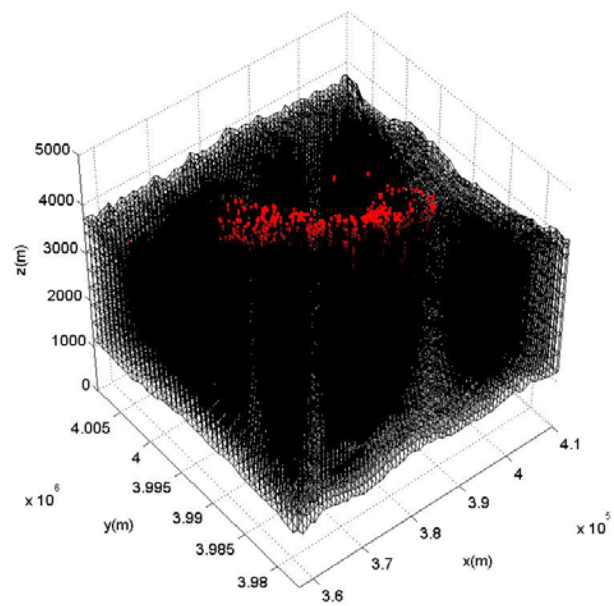

Fig.6. Spatial location of Boreholes and the structure

Afterwards, data from surveying line were assigned to the model similarly. There are 16 shallow artificial earthquake surveying lines provided by the Lanzhou earthquake administration used, which are distributed upon six main faults in the working area. Among the 16 surveying lines, one is shallow artificial refraction ray and the rest 15 are controlled exploration rays.

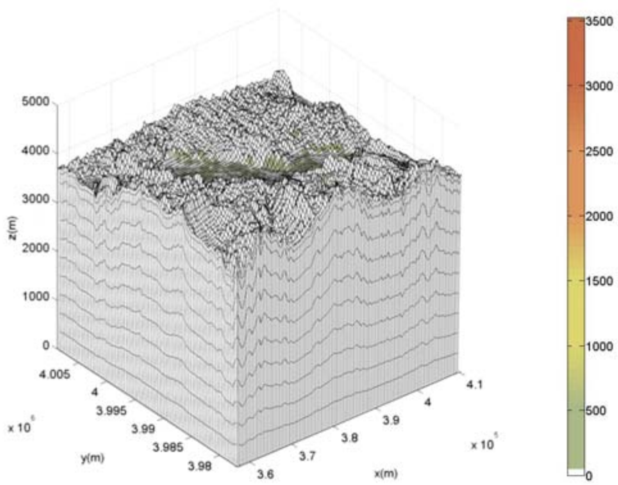

Fig.7. 3D velocity model assigned with borehole data

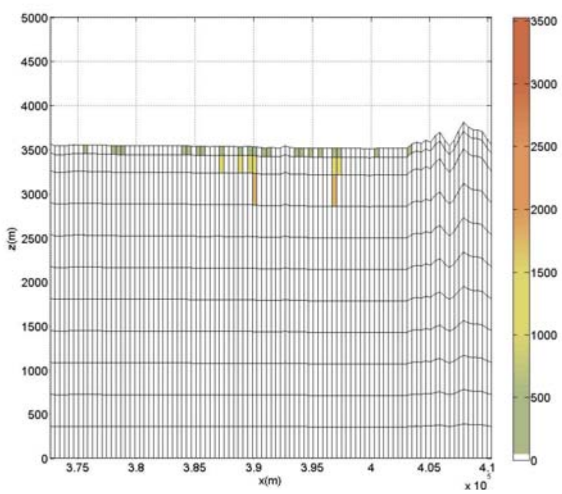

Fig.8. profile at section 1-1

The location of surveying lines in the working area are shown in figure 9 together with their names, and the spatial relative location of surveying lines in the structure model are shown in figure 10. Only the upper three layers shown in figure 10 because all the surveying lines are distributed there. Similar to

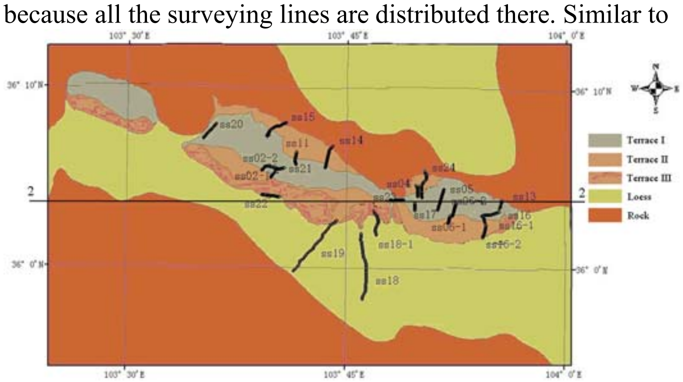

Fig.9. Ichnography of surveying line distribution

the boreholes, one element may be assigned with several surveying line data, and the mean of these data would be computed to be the velocity of the element for this case. The structure model in figure 7 after assignment with surveying line data was illustrated in figure 11. Also, the profile of section 2-2 in figure 9 is shown in figure 12 to exhibit the inner structure of the model after assignment.

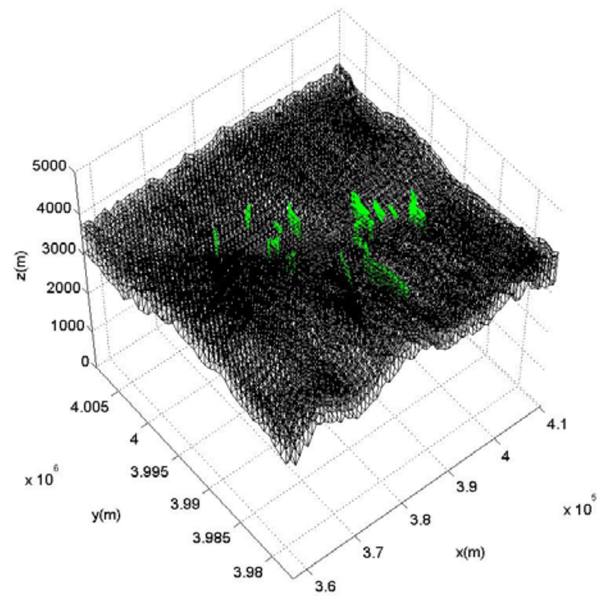

Fig.10. Spatial location of surveying lines and the upper three finite element layers

As seen in figure 7 and figure 11, most of the elements in the structure model still lack of shear wave velocity after the two-steps assignment. Kriging interpolation method based on the spherical variation function model was employed for those finite elements, and dummy boreholes were also used to improve the validity of the interpolation based on sparse data. Shear wave velocity data from seismic array were used to control the velocities of dummy boreholes and limit the velocities from interpolation. Control values specified from seismic array data for each layer of the model are listed in table 1.

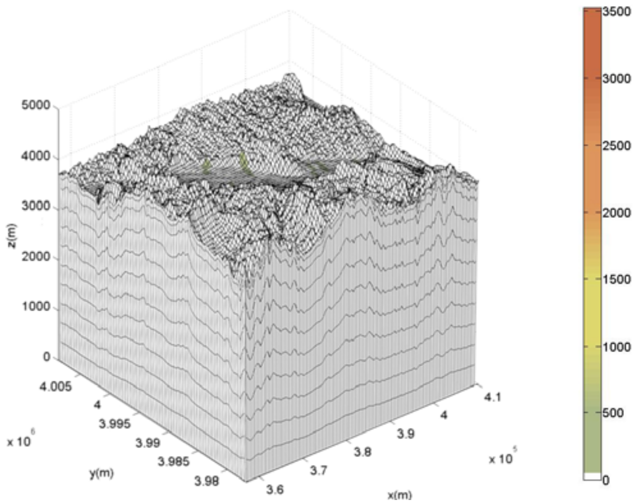

Fig.11. 3D velocity model assigned with surveying line data

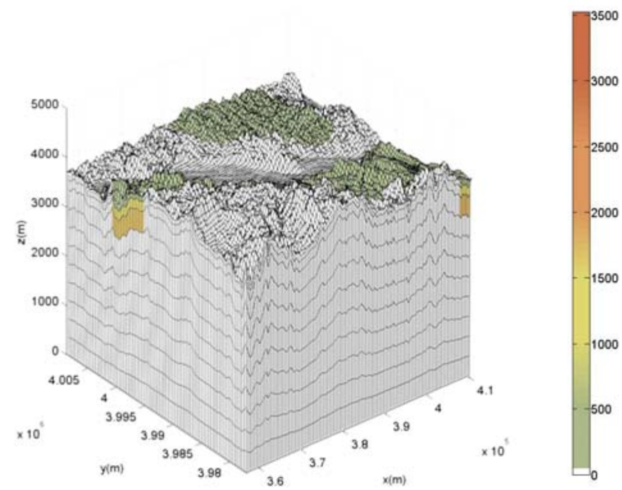

Fig.13. Interpolation result of loess bench

For the interpolation at the upper three layers where the shear wave velocity changes rapidly, the working area was divided into five sub-areas, for which the interpolation was preformed separately. Sub-areas were defined according to different geological conditions as shown in figure 2. For each of the rest layers (e.g. about 700 meters deeper), there barely have large inhomogeity in the medium, and could be considered as layered medium and interpolated in the whole layer. For illustration, figure 13 and 14 give the shear wave velocity for the loess site and rock site at the upper three layers.

Finally, interpolation results in these sub areas were merged after smoothing the interfaces of sub areas to form the final 3D shear wave velocity structure model, as illustrated in figure 15.

Fig.4-8 Location of the section 1-1

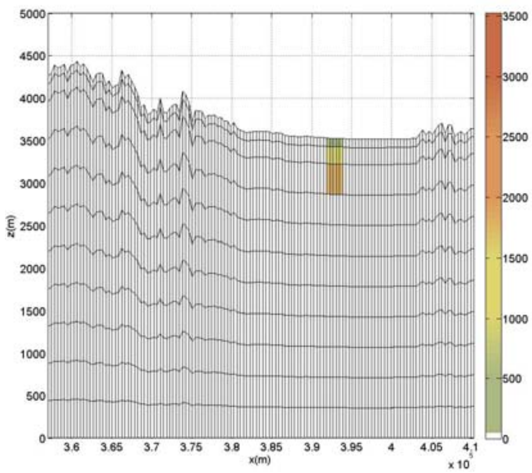

Fig.12. profile at of section 2-2

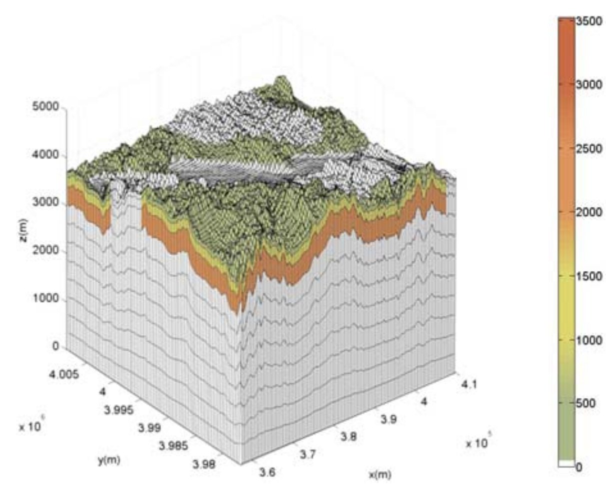

Fig.14. Interpolation result of rock

Table 1 Control values of shear wave velocity in the 3D finite element model

1	2	3	4	5	6	7	8	9	10	11
700	1490	2280	3070	3136	3200	3266	3330	3393	3460	3522

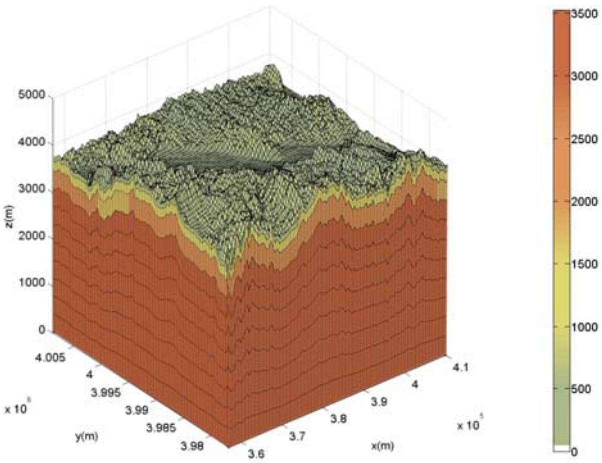

Fig.15. 3D velocity structure of the working area

LONG-PERIOD GROUND MOTION SIMULATION

The model obtained in the previous section was applied to the long-period ground motion simulation of the Lanzhou basin and its vicinity. The Maxianshan Northern fault was assumed to be the causative fault, and the presumed magnitude was 6.5. The fault is sinistral strike-slip fault with orientation of strike 130°and dip 76°. The dimension and slip distribution of the Maxianshan Northern fault was adopted from a past work (Tao *et al*, 2007), as shown in figure 16, and the relative location of the fault and the working area was illustrated in figure 17.

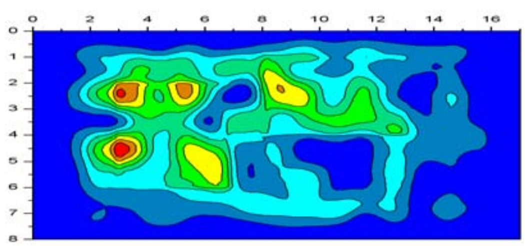

Fig.16. finite fault source model

The simulation is by means of the Numerical Green's function approach introduced in previous section (Zhang, 2005). Seven representative points were picked out according to the PGA zoning map acquired by high-frequency ground motion synthesis as illustrated in figure 18. Seen from figure 18, the whole working area was divided into five PGA zones and two geological zones. Seven points marked with green stars were

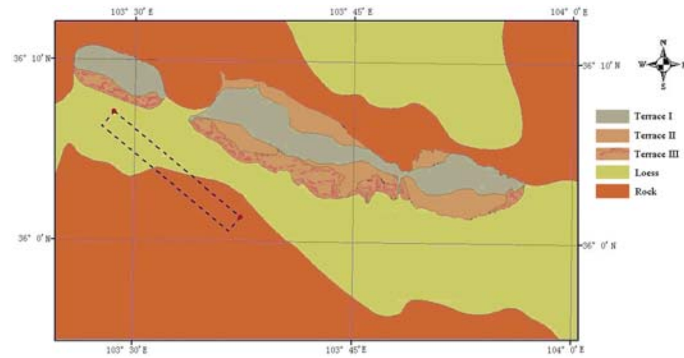

Fig.17. Locations of the fault and the basin

picked out for almost each PGA zone and each geological zone. Ground motion time histories at the seven represented points were compared with those based on a horizontal layered velocity structure model (Tao *et al*, 2007), as figure 19 shows.

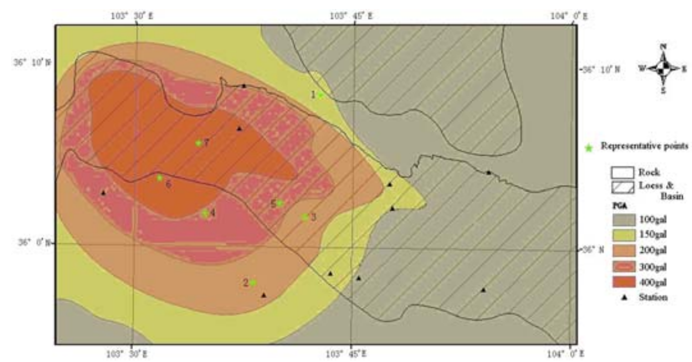

Fig.18. locations of the seven representative points

Seen from figure 19, the peak of the time history by 3D velocity model for number 3, 5 and 7 approaches that by horizontal layered velocity model, but the waveform of the former is more complex than that of the latter. By contrast, for number 1, 2, 4 and 6, both the peak and the waveform of the time history by 3D velocity model are much different than those by horizontal layered velocity model. For further analysis, the shear wave velocity of the upper three layers of the 3D velocity model and of the horizontal layered velocity model, where includes most of the borehole and survey line data, are listed in Table 2. From Table 2, one may observe that velocity in the horizontal layered model is lower than that in the 3D velocity model. This is because the velocity of the layer in the horizontal layered model is determined by the borehole and survey line data in this layer. From figure 5 and 9, most of these data are collected from the basin. Layer velocity determined from these data must lead to the underestimation on the velocity of the rock site in the layer,

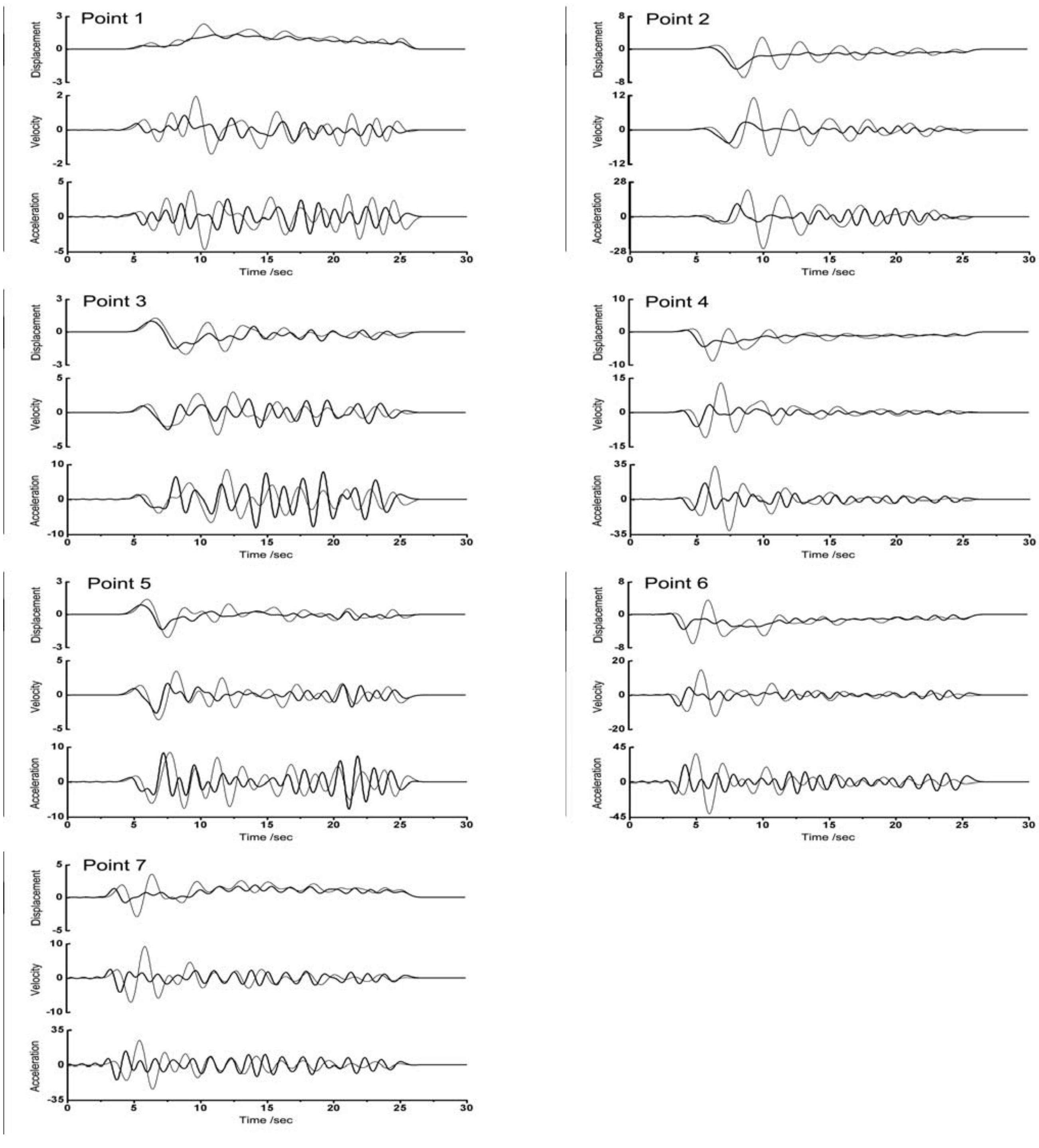

Fig.19. Ground motions at seven representative points (Heavy lines for 3D model and Light lines for Horizontal layered model)

and hence lead to the overestimation on the long-period ground motion, which could also be observed in figure 19.

Table 2. Shear wave velocities at the 7 points in the two models

Layer	Velocity Model	1	2	3	4	5	6	7
1	3D	693	700	483	690	478	686	478
	Horizontal layered	217	217	217	217	217	217	217
2	3D	1343	1346	1016	1346	1022	1345	1006
	Horizontal layered	754	754	754	754	754	754	754
3	3D	2143	2150	1715	2140	1698	2136	1655
	Horizontal layered	2407	2407	2407	2407	2407	2407	2407

CONCLUSION

In this paper, a procedure to build up 3D shear wave velocity structure model is introduced briefly based on the example of the Lanzhou basin. The model developed was hence employed to calculate the ground motion time histories at the 10854 surface points of the working area by means of a simplified Numerical Green function approach. Ground motion time histories at seven represented points were picked out and compared with those from a horizontal layered velocity structure model built for the same working area to validate the reliability and availability of the 3D velocity structure model developed herein. For a large site, especially that including multiple geological conditions such as terrace, loess and rock and so forth, the underground medium varies significantly not only along the deep direction but also along the horizontal direction. Traditional velocity model, such as 1D or horizontal layered model, may result in the oversimplification on the site condition and the underestimation on the shear-wave of the site, and hence affect the accuracy of the finite element calculation. Further study on improving the procedure for a more accurate 3D shear-wave velocity model will be preformed and presented elsewhere.

ACKNOWLEDGEMENTS

This work was supported by National Key Project of Scientific and Technical Supporting Programs from the Ministry of Science & Technology of China under Contract No.2006BAC13B02, and National Nature Science Foundation of China under Contract No. 50778058 and 90715038.

REFERENCES

Graves R. W., A. Pitarka and P. G. Somerville (1998). Ground motion amplification in the santa monica area: effects of shallow basin edge structure. Bull Seism Soc Amer, Vol. 88, 1224-1242

Liao Z. P., et al (2002). Stable implementation of transmitting boundary in numerical simulation of wave motion. Chinese Journal of Geophysics, Vol. 45(4), 533-545

Magistrale H., K. McLaughlin and S. Day (1996). A geology based 3d velocity model of the Los Angeles basin sediments. Bull Seism Soc Amer, Vol. 86, 1161-1166

Olsen K. B. (2000). Site Amplification in the Los Angeles Basin from 3D Modeling of Ground Motion. Bull Seism Soc Amer, Vol. 90, 77-94

Shi L J (2007). Exploration and Imaging of 3D Subsurface Velocity Structure by Microtremors. Ph.D. Dissertation, Institute of Engineering Mechanics China Earthquake Administration, Harbin, China (in Chinese)

Tao X X, Sun X D, et al (2007). Seismic hazard assessment of active faults in Lanzhou City. Harbin, Harbin Institute of Technology (in Chinese)

Zhang D. L. (2005). Simulation of long period strong ground motion at near-field by numerical Green function method. Ph.D. Dissertation, Institute of Engineering Mechanics China Earthquake Administration, Harbin, China (in Chinese)

Zhang D.L., X.W. Xu, B.M. Zhao, G. H. Chen and T. W. Xie (2007). 3-D physical model in strong ground motion numerical simulation: a case study of Kunming basin. ACTA. 29(2):187-196